Computational and Theoretical Chemistry 1247 (2025) 115138

Contents lists available at ScienceDirect

Computational and Theoretical Chemistry

journal homepage: www.elsevier.com/locate/comptc

Quantum-chemical insights into the thermodynamic and electronic characteristics of monoterpene hydrocarbons

Maria Milena Regina E. Cavalcante [a], Rosemarie B. Marques [b], Ricardo R. Martins [c], Evandro Paulo S. Martins [d], Agmael M. Silva [c], Marcelo L. Pereira Jr. [e,*], Antonio de Macedo-Filho [a,f]

[a] State University of Piauí, PPGQ-GERATEC, Teresina, PI, Brazil
[b] State University of Piauí, Biotechnology and Biodiversity Research Center, Teresina, PI, Brazil
[c] Federal Institute of Education, Science and Technology of Piauí, Teresina, PI, Brazil
[d] State University of Piauí, Campus Prof. Antonio Geovanne Alves de Sousa, Piripiri, PI, Brazil
[e] University of Brasília, College of Technology, Department of Electrical Engineering, Brasília, DF, Brazil
[f] State University of Piauí, Department of Physics, Teresina, PI, Brazil

ARTICLE INFO

Keywords:
Quantum-descriptors
Electronic properties
Thermodynamic properties
Density Functional Theory
Pharmacology application

ABSTRACT

The monoterpene hydrocarbons limonene, sabinene, α-phellandrene, and β-phellandrene are organic compounds produced by plants during adaptation, defense, and reproduction processes, with their concentrations varying according to physical and chemical factors. These compounds were identified as the group with the highest percentage in the essential oil of the leaves of *Croton heliotropiifolius* Kunth, whose extract shows potential as a drug candidate. To better understand these compounds' properties, we studied the quantum-chemical descriptors of these four molecules. In addition, thermodynamic and electronic properties of the chemical structures of the monoterpene hydrocarbons were obtained using the Density Functional Theory (DFT) formalism. This study provides new insights into the analyzed systems. It establishes correlations between structure, property, and activity, allowing the investigated monoterpene compounds to be screened and selected for the design of future drugs based on essential oils derived from these molecules. It also assists in identifying ideal preparation and administration methods for your products suitable for outpatient, hospital, and home use.

1. Introduction

The medicinal properties exhibited by various plant species are associated with chemical compounds they produce for adaptation, defense, and reproduction [1]. Many of these properties were empirically observed and used in attempts to relieve pain and treat diseases, even without a clear understanding of their mechanisms of action [2]. This empirical knowledge laid the foundation for the arsenal of drugs available today [3].

In this context, the species *Croton heliotropiifolius* Kunth, an endemic plant from northeastern Brazil commonly known as "velame", has gained scientific attention. It is widely used in traditional medicine for treating colds, pain, inflammation, fungal infections, gastrointestinal disorders, and diabetes [4–7]. These applications have motivated the investigation of its essential oil, which predominantly contains organic compounds such as limonene,[1] sabinene,[2] α-phellandrene,[3] and β-phellandrene.[4]

These four compounds have been widely studied for their pharmacological potential, exhibiting antimicrobial, anti-inflammatory, and antioxidant properties [4,5,7]. Their presence in medicinal plants and essential oils has been associated with potential therapeutic effects, making them valuable candidates for drug discovery and rational molecular design [8,9]. Understanding their quantum-chemical descriptors provides key insights into their physicochemical and electronic properties, influencing their interaction with biological receptors and their potential efficacy in pharmacological applications.

In this perspective, scientific evidence suggests the potential of these compounds for developing novel drugs to treat various diseases,

* Corresponding author.
E-mail address: marcelo.lopes@unb.br (M.L. Pereira Jr.).

[1] 4-isoprenyl-1-methylcyclohexene
[2] (1R,5R)-4-methylene-1-propan-2-ylbicyclo[3.1.0]hexane
[3] 2-methyl-5-propan-2-ylcyclohexa-1,3-diene
[4] 3-methylene-6-propan-2-ylcyclohexene

https://doi.org/10.1016/j.comptc.2025.115138
Received 26 November 2024; Received in revised form 6 February 2025; Accepted 7 February 2025
Available online 15 February 2025

expanding therapeutic options, and opening pathways for the development of model medications [8]. However, the refinement or introduction of new drugs involves stringent efficacy and safety standards, which demand significant time, resources, and cost, primarily due to the low success rates from initial planning to market approval [9].

The challenges in identifying active compounds delay the treatment of numerous diseases, limiting therapeutic options and reducing survival rates [10]. In this regard, theoretical studies supported by computational tools play a pivotal role in rational drug design [4, 11,12]. These approaches enable extensive and realistic analyses of complex systems in less time and at a lower cost. They facilitate understanding chemical structures, properties, and potential mechanisms of action, optimizing molecular interaction studies and reducing waste generation [13].

In this work, we employed computational quantum chemistry methods to investigate the properties of limonene, sabinene, α-phellandrene, and β-phellandrene. The combination of quantum-chemical descriptors with pharmacokinetic and toxicological data [9] provides an essential framework to describe the interactions of these molecules with biological receptors and to analyze the correlations between chemical structure, biological activity, and physicochemical properties. To achieve this, we calculated descriptors such as electric dipole moment, charge density, electrostatic potential maps, frontier orbital energies (HOMO-LUMO), ionization potential, electron affinity, electronegativity, hardness, softness, chemical potential, and polarizability. Thermodynamic parameters, including free energy, enthalpy, and entropy, were also obtained, alongside the total and projected density of states for the optimized chemical structures of these monoterpenes, using Density Functional Theory (DFT) formalism [12–14]. This study enhances understanding of the analyzed molecules and identifies correlations between structure, property, and activity, enabling their evaluation and selection based on desired traits. These findings contribute to the rational design of future drugs derived from this essential oil. They inform its products' optimal preparation and administration methods, with potential applications in ambulatory, hospital, and home-care settings.

2. Computational methodology

To investigate the physicochemical characteristics of the monoterpene hydrocarbons limonene, sabinene, α-phellandrene, and β-phellandrene, present in the leaves of *Croton heliotropiifolius* Kunth, theoretical calculations were performed using DFT as implemented in the ORCA and Quantum ESPRESSO (QE) computational packages. The atomic coordinates of each structure were retrieved from the PubChem database [15].

For molecular properties, we employed the B3LYP hybrid exchange–correlation functional, which provides a reliable balance between accuracy and computational cost for organic molecules. The def2-TZVPP basis set was chosen to describe electron correlation effects with high precision. To improve computational efficiency, the resolution-of-identity (RI) approximation was applied using the def2/J auxiliary basis set.

The self-consistent field (SCF) equations were iteratively solved for each monoterpene, with an energy convergence threshold of 6.8×10^{-8} eV. Based on the optimized geometries, molecular properties were obtained, including charges (Mulliken, NPA, NBO, Chelpg), resultant dipole moment, frontier orbital energies, electrostatic potential maps, thermodynamic parameters, and polarizability.

Thermodynamic parameters, including free energy, enthalpy, and entropy, were obtained using the harmonic approximation within the DFT formalism. These values correspond to the isolated gas-phase molecules at 298.15 K and 1 atm, considering equilibrium geometries optimized at the B3LYP/def2-TZVPP level of theory.

For total and projected density of states (DOS/PDOS) calculations, the QE package was used with the Perdew–Burke–Ernzerhof (PBE) exchange–correlation functional within the generalized gradient approximation (GGA), which is widely applied in electronic structure calculations. The plane-wave basis cutoff was set to 25 eV, and the Brillouin zone was sampled using a Γ-point Monkhorst–Pack grid. A self-consistent field energy convergence criterion of 10^{-6} eV was adopted.

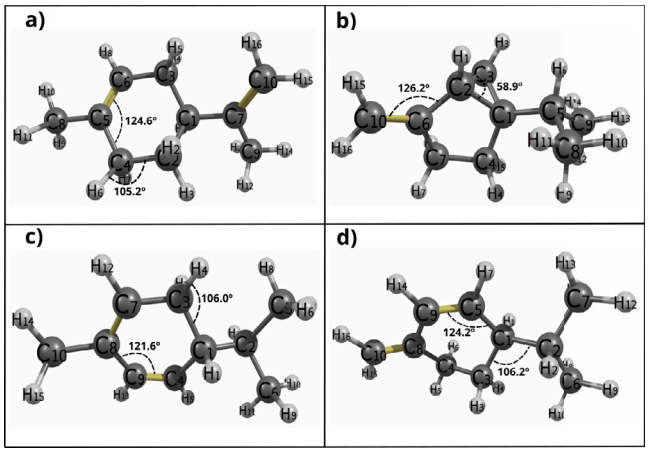

Fig. 1. Schematic representation of the optimized molecules of limonene (a), sabinene (b), α-phellandrene (c), and β-phellandrene (d), highlighting atomic nomenclature and related angles.

All calculations were performed in the gas phase, and solvent effects were not considered. While this approach allows for a fundamental understanding of monoterpene properties, future studies incorporating explicit solvent models or condensed-phase simulations may provide further insights into their behavior in biological environments.

3. Results and discussion

This section presents the results of quantum chemical simulations, focusing on monoterpene hydrocarbons' thermodynamic and electronic properties based on the methodology discussed in the previous section.

3.1. Structural details

The molecular structure of the monoterpene hydrocarbons limonene, sabinene, α-phellandrene, and β-phellandrene consists of 26 atoms, with the chemical formula $C_{10}H_{16}$. Fig. 1 shows the optimized conformations of each investigated molecule, configuring them as nonlinear structures with predominantly covalent bonds of σ and π types, described as σ (C – sp^3 and H – 1s), σ (C – sp^3 and C – sp^3), σ (C – sp^2 and C – sp^2), and π (C – 2p and C – 2p), resulting from the frontal combinations of sp^3 and sp^2 hybrid orbitals and the parallel combinations of pure p orbitals, respectively. The figure also highlights the angles between the orbitals, which range from 105.2° to 124.6° (limonene), 58.9° to 125.2° (sabinene), 106.6° to 123.5° (α-phellandrene), and 106.2° to 124.2° (β-phellandrene), indicating the presence of sp^3 and sp^2 hybridizations. Table S1 (supplementary material) shows each molecule's calculated bond angles.

Regarding the structural organization of the monoterpenes found in the leaves of *Croton heliotropiifolius* Kunth, the average bond lengths are approximately 1.33 Å for the C=C double bonds and 1.54 Å for the C–C single bonds, which is in agreement with experimental values reported for these bond types. Additionally, the average C–H bond lengths observed were around 1.10 Å. Table S2 (supplementary material) presents all the bond lengths for limonene, sabinene, α-phellandrene, and β-phellandrene. Small rotations were also observed in the bonds C_1-C_7, C_1-C_2, C_1-C_3, C_4-C_2 in limonene; C_7-C_4, C_4-C_1, C_1-C_5 in sabinene; C_4-C_3, C_1-C_3, C_1-C_2 in β-phellandrene; and C_2-C_1, C_3-C_1 in α-phellandrene, with their structural characteristics maintained in terms of bond length.

Table 1
Coordinates of the electric dipole moment vectors calculated using the Mulliken method.

Monoterpene	Limonene	Sabinene	α-phellandrene	β-phellandrene
x (Å)	−0.101	0.336	0.071	0.301
y (Å)	−0.195	0.015	0.038	−0.124
z (Å)	−0.167	−0.112	−0.004	−0.049
Magnitude	0.702	0.901	0.205	0.838

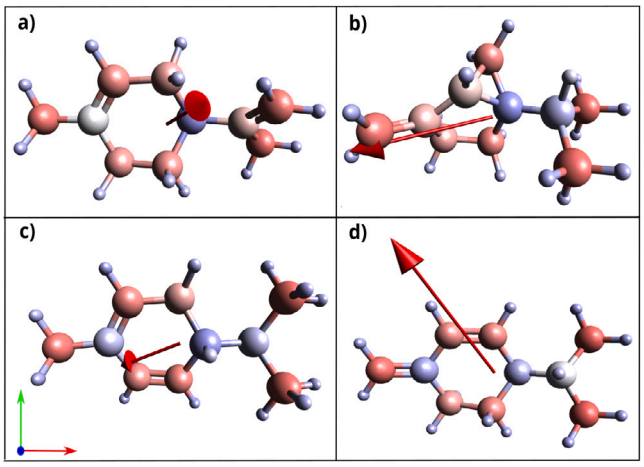

Fig. 2. Resulting electric dipole moment vector (origin coinciding with the center of mass) and partial atomic charges, obtained using the Mulliken method, of the optimized chemical structures of limonene (a), sabinene (b), α-phellandrene (c), and β-phellandrene (d). Atomic charges are indicated by color shades, with negative charges in red and positive charges in blue.

Furthermore, it was observed that the structures exhibit optical isomerism due to the presence of the asymmetric carbon C_1, resulting in the dextrorotatory and levorotatory species [16]. Although these species have the same molecular formula, they differ in the spatial arrangement of ligands around the chiral carbon and are non-superimposable mirror images. However, they present identical physicochemical properties but exhibit distinct chemical behaviors in chiral environments.

This behavior is particularly relevant in biological interactions, as most molecular drug targets, such as membrane proteins and enzymes, are chiral compounds, influencing the efficacy or toxicity of the drug. Therefore, when a racemic mixture is used as a medication, conducting chemical and toxicological tests for each enantiomer is crucial, as comparing them to the racemic mixture [17].

3.2. Polarity

In drug design, it is crucial to consider polarity, as this property determines solubility and directly influences pharmacokinetic characteristics. To this end, the polarity of the molecules investigated here was determined based on the calculation of the resulting electric dipole moment vectors, with origins coinciding with the following centers of mass: limonene (0.009, 0.031, 0.015), sabinene (0.086, −0.062, −0.011), α-phellandrene (0.085, 0.020, −0.055), and β-phellandrene (0.108, −0.041, 0.023). The x, y, and z coordinates and the magnitudes of the resulting electric dipole moment vectors are presented in Table 1. The position of these vectors relative to the molecules is shown in Fig. 2.

Analyzing the obtained values, it can be concluded that all omolecules exhibit slight polarity, as the sum of the electric dipole moment vectors of the polar covalent bonds is non-zero. This indicates that these molecules, such as water, are weakly soluble in polar solvents (lipophilic). Dipole formation in these molecules arises from charge displacement due to differences in electronegativity between the atoms involved in these bonds.

Moreover, the slight polarity of these molecules suggests that they are soluble in nonpolar or low-polarity solvents. The solubilization process is effective if the energy from establishing new interactions is sufficient to overcome the initial interactions.

Finally, examining the direction of the resulting dipole vectors in sabinene, α-phellandrene, and β-phellandrene reveals that the left regions of the molecules are more positive, which aligns with the electrostatic potential map (see Fig. 3), making these regions susceptible to reactions or interactions with nucleophiles. On the other hand, the cyclic regions concentrate higher electron density and are therefore more negative. For limonene, the resulting vector indicates the right area as the most positive [18].

3.3. Charge density

Ligand–receptor interactions are strongly influenced by electrostatic effects. The chemical behavior of a molecule and its reactive sites for electrophilic and nucleophilic interactions can be characterized by charge distribution obtained through various computational methods. In this study, we employed Mulliken Charges from Electrostatic Potentials using a Grid-based (CHELPG), Natural Population Analysis (NPA), and Natural Bond Orbital (NBO) methods [12,19] to estimate the atomic charge densities of monoterpene hydrocarbons, using the B3LYP functional and the def2-TZVPP basis set. Each compound's total atomic charge summation was consistent with the overall molecular charge. For limonene and sabinene, most carbon atoms followed the charge trend NBO < NPA < Mulliken < CHELPG, while for α-phellandrene and β-phellandrene, the trend was NBO = NPA < Mulliken < CHELPG (see Table 2).

The NBO-derived charges were generally lower than those from other methods, indicating a more accurate representation of bonding interactions. This trend is expected as NBO incorporates delocalization effects more effectively. In contrast, Mulliken and NPA methods, which partition the molecular wavefunction into atom-centered basis functions, can introduce charge deviations due to their neglect of electronegativity effects [18].

The analysis of regions with higher electronic density reveals that, for atoms involved in the bonds $C_5{=}C_6$ and $C_7{=}C_{10}$ in limonene and $C_{10}{=}C_6$ in sabinene, only the charge signs of C_7 (limonene) and C_6 (sabinene) obtained by the Mulliken method differ from the other methods. For α-phellandrene and β-phellandrene, the regions of higher electronic density are associated with the bonds $C_8{=}C_7$ and $C_9{=}C_4$, and $C_9{=}C_5$ and $C_{10}{=}C_8$, respectively. In these regions, a charge sign inversion occurs only for atom C_8 according to the NPA method, a result also confirmed by NBO, reinforcing the reliability of this observation. The atomic charges estimated by the four methods adequately reproduce the electrostatic potential map of the analyzed molecules, with significant divergences only for C_5 in limonene and C_2 in sabinene.

Mulliken population analysis further indicates that the hydrogen atoms in β-phellandrene (Table S3, see Supplementary Material) exhibit, on average, more positive charges compared to other molecules, indicating higher acidity. In contrast, limonene presents the lowest charge values for these atoms. In the $C_5{=}C_6$ and $C_7{=}C_{10}$ bonds of limonene, carbons C_5 and C_7 each hold approximately six electrons, suggesting a higher propensity for nucleophilic attacks. Their adjacent atoms, C_6 (6.17e) and C_{10} (6.24e), display similar electronic populations, considering a total of 76 electrons in the molecule. For α-phellandrene and β-phellandrene, atoms C_7 (6.16e) and C_{10} (6.37e) show higher electronic density in the analyzed regions compared to adjacent atoms C_8, corroborating the electrostatic potential map information. In sabinene, the analysis identifies C_{10} as the site of the highest electronic density in the $C_{10}{=}C_6$ bond.

Table 2
Atomic charges for carbon atoms calculated using Mulliken, CHELPG, NPA, and NBO methods for limonene, sabinene, α-phellandrene, and β-phellandrene, employing the B3LYP functional and def2-TZVPP basis set.

Atoms	Limonene				Sabinene				α-Phellandrene				β-Phellandrene			
	Mull	NPA	CHELPG	NBO	Mull	NPA	CHELPG	NBO	Mull	NPA	CHELPG	NBO	Mull	NPA	CHELPG	NBO
C_1	0.138	−0.239	0.078	−0.240	0.146	−0.013	0.092	−0.016	0.138	−0.242	0.179	−0.244	0.075	−0.249	0.343	−0.251
C_2	−0.160	−0.366	0.018	−0.366	−0.022	−0.258	−0.080	−0.259	0.048	−0.189	0.365	−0.191	0.003	−0.188	0.330	−0.190
C_3	−0.101	−0.414	0.273	−0.415	−0.206	−0.402	−0.330	−0.402	−0.090	−0.418	0.310	−0.417	−0.205	−0.371	0.011	−0.371
C_4	−0.132	−0.420	0.025	−0.420	−0.197	−0.384	−0.012	−0.384	−0.211	−0.146	−0.253	−0.145	−0.127	−0.414	0.099	−0.412
C_5	0.001	0.012	0.111	0.007	0.060	−0.194	0.277	−0.195	−0.301	−0.590	−0.227	−0.590	−0.193	−0.147	0.333	−0.146
C_6	−0.175	−0.188	−0.405	−0.188	−0.069	0.032	0.163	0.028	−0.293	−0.587	−0.215	−0.587	−0.358	−0.591	−0.256	−0.590
C_7	−0.041	0.045	0.108	0.041	−0.104	−0.430	−0.027	−0.431	−0.201	−0.162	−0.445	−0.161	−0.349	−0.588	−0.278	−0.587
C_8	−0.262	−0.611	−0.209	−0.610	−0.303	−0.589	−0.243	−0.589	0.046	−0.043	0.260	−0.047	0.092	−0.025	0.177	−0.027
C_9	−0.278	−0.622	−0.124	−0.622	−0.306	−0.587	−0.217	−0.586	−0.172	−0.224	−0.176	−0.224	−0.167	−0.223	−0.146	−0.223
C_{10}	−0.242	−0.411	−0.480	−0.409	−0.263	−0.414	−0.506	−0.413	−0.261	−0.607	−0.242	−0.606	−0.294	−0.376	−0.495	−0.374

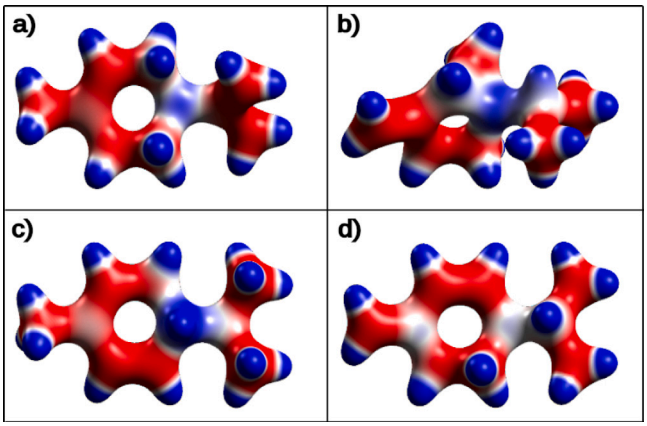

Fig. 3. EPMs of the optimized chemical structures of the hydrocarbon monoterpenes limonene (a), sabinene (b), α-phellandrene (c), and β-phellandrene (d).

3.4. Electrostatic potential maps

Electrostatic potential maps (EPMs) are essential for predicting possible interaction sites between molecules and ligands. In this study, the EMPs of each investigated molecule were analyzed. Fig. 3 displays these EMPs, where the blue and red regions indicate positive and negative charge density, respectively [20].

Negatively charged areas are the regions of interest for reactivity, as these are the most likely sites for effective chemical interactions with cationic ligands. In this context, the most favorable areas are those with minimal steric hindrance and high negative charge density. Double bonds are particularly significant, as they exhibit higher electron density than single bonds, owing to the sharing of four electrons versus two in single bonds.

Additionally, the π-electrons in double bonds are more accessible to approaching molecules since they are located above and below the plane of the double bond, unlike single bonds where electrons are shielded between nuclei. Consequently, in potential reactions, an electrophile would initially add to one of the alkene's sp^2 carbons, followed by adding a nucleophile to the other sp^2 carbon.

For limonene, the sp^2 carbons are located in the $C_5=C_6$ and $C_7=C_{10}$ bonds. The electron cloud is more concentrated in these regions, resulting in partial negative charges. Among these carbons, C_5 and C_7 are the most favorable for nucleophilic attacks, as the reaction's intermediate would involve the formation of tertiary carbocations, which are more stable and require less energy to form. The tertiary carbocation would react with a nucleophile from the ligand in the second reaction step. Conversely, C_6 and C_{10} are more susceptible to electrophilic attacks.

For the other molecules, potential interaction sites include $C_{10}=C_6$ (sabinene), $C_8=C_7$ and $C_9=C_4$ (α-phellandrene), and $C_9=C_5$ and $C_{10}=C_8$ (β-phellandrene). Among these, the carbon most vulnerable to nucleophilic attack due to forming a tertiary carbocation is C_8 in both α- and β-phellandrene. For C_9 and C_4 in α-phellandrene, as well as C_9 and C_5 in β-phellan−drene, no significant difference exists regarding which carbon the electrophile or nucleophile will bind to, given their identical substituents. In sabinene, the carbon C_6 is prone to electrophilic attack, as the electron cloud is more concentrated at this site, resulting in a partial negative charge. This occurs because the alkyl substituents attached to C_6 reduce the positive charge concentration on this carbon.

3.5. Frontier molecular orbitals

The highest occupied molecular orbitals (HOMO) and the lowest unoccupied molecular orbitals (LUMO) are critical for understanding the mechanism of chemical reactions, as they are the orbitals that interact to form and break bonds. When two reactant species approach, electrons flow from the HOMO of one species to the LUMO of the other.

Identifying electrophilic and nucleophilic regions is essential for predicting molecular interactions and reactivity. While global descriptors such as ionization potential, electron affinity, and electronegativity provide valuable insights, local conceptual DFT descriptors can offer a more spatially resolved approach to characterizing reactive sites [21]. In this study, we focused on frontier orbital analysis and electrostatic potential maps to assess these properties, ensuring a broad characterization of electronic reactivity.

Fig. 4 shows the spatial distribution of the frontier orbitals for limonene, sabinene, α-phellandrene, and β-phellandrene. The red and blue colors represent the negative and positive phases of the molecular orbital wavefunction, respectively, corresponding to the regions where electrons are likely to be found. It is noteworthy that the orbitals of atoms C_{10}, C_7, C_1, C_3, C_6, C_5, C_4, C_8, H_5, H_4, H_7, H_6, H_9, and H_{11} in limonene, C_{10}, C_6, C_7, C_2, C_1, C_4, C_3, C_5, C_9, H_{13}, H_2, H_3, H_1, H_8, H_7, H_4, and H_5 in sabinene, C_{10}, C_8, C_7, C_9, C_3, C_4, C_1, C_2, H_{16}, H_{15}, H_3, H_4, and H_1 in α-phellandrene, and C_{10}, C_8, C_9, C_4, C_5, C_3, C_1, C_2, H_6, and H_1 in β-phellandrene contribute to the formation of the HOMO. Asymmetrical distributions of positive and negative phases are observed at atoms C_3 and C_4 in limonene, C_7, C_4, C_1, C_3, C_5, and C_9 in sabinene, C_3 and C_1 in α-phellandrene, and C_4, C_3, C_1, and C_2 in β-phellandrene.

Regarding the formation of the LUMO, the atoms C_{10}, C_7, C_9, C_1, C_3, C_2, C_6, C_4, C_5, H_{13}, H_{12}, H_5, H_4, H_7, H_6, H_9, and H_{11} in limonene, C_{10}, C_6, C_7, C_2, C_1, C_4, C_3, C_9, H_8, H_7, H_1, and H_3 in sabinene, C_{10}, C_8, C_7, C_9, C_3, C_4, C_1, C_2, H_{16}, H_{15}, H_{13}, H_3, H_4, and H_1 in α-phellandrene, and C_{10}, C_8, C_9, C_5, C_3, C_1, C_2, C_6, H_6, and H_1 in β-phellandrene contributed to the constitution of the LUMO, with noticeable asymmetry in the positive and negative phases, especially at atoms C_2 (limonene), C_3, C_1, and C_4 (sabinene), C_3 and C_1 (α-phellandrene), and C_3 (β-phellandrene).

Through the spatial distribution, it was also possible to observe that both the HOMO and LUMO orbitals have bonding and antibonding regions. However, in the HOMO, bonding orbitals dominate, while

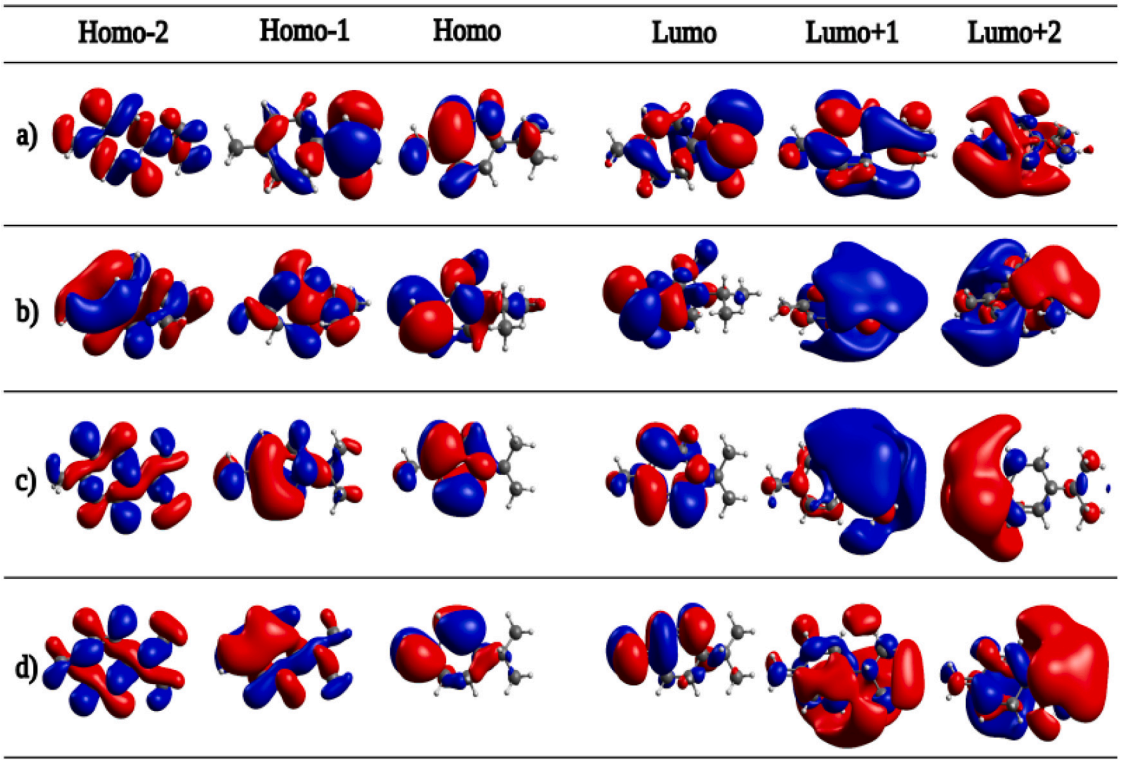

Fig. 4. Molecular orbital series of HOMO-LUMO for the chemical structures of limonene (a), sabinene (b), α-phellandrene (c), and β-phellandrene (d).

antibonding orbitals predominate in the LUMO. In this context, it is considered that electrons occupying bonding orbitals (around 99%) are more likely to be found in the internuclear region, making these portions more susceptible to electrophilic attacks. On the other hand, electrons occupying antibonding orbitals (around 1%) are located in external areas to the nuclei of the atoms involved in bonding, suggesting that electron population in the regions between the nuclei of bonding atoms is lower, thus making them more vulnerable to nucleophilic attacks.

In general, the formation of molecular orbitals is influenced by the extent of interaction between atomic orbitals, with stronger bonds arising from more significant overlap. Therefore, factors such as bond distance, electronegativity of the atoms involved, orbital interaction geometry, and orbital energy levels will affect the bond strength. Another critical factor is that atomic orbitals combine more effectively when their energies are similar [22,23].

However, the HOMO or LUMO orbitals may not be suitable for a given reaction due to their spatial extent, symmetry, or nodal properties [22]. In such cases, the following orbital or any orbital with energy close to the HOMO or LUMO may be used. A portion of the HOMO-LUMO series for the analyzed structures is shown in Fig. 4. Thus, the responsibility for molecular reactivity rests with the HOMO-LUMO orbitals and those adjacent to them. Therefore, the HOMO-LUMO series should be considered within the context of reactivity arguments. Table 4 presents the energy values for the HOMO and LUMO molecular orbitals, as well as for their respective neighbors: HOMO-2, HOMO-1, LUMO+1, and LUMO+2. Additionally, as highlighted in Table 4, the energy gap between the HOMO-LUMO for each molecule is as follows: 6.67 eV for limonene, 6.58 eV for sabinene, 5.04 eV for α-phellandrene, and 5.36 eV for β-phellandrene.

These values are in reasonable agreement with previously reported theoretical studies. Oses et al. [24] calculated the HOMO-LUMO gap as 5.46 eV for α-phellandrene and 5.77 eV for β-phellandrene, which are slightly higher than our computed values of 5.04 eV and 5.36 eV, respectively. Similarly, Zeinali et al. [25] reported band gaps of 6.37 eV for limonene and 6.25 eV for sabinene, compared to our values of 6.67 eV and 6.58 eV. The discrepancies between our results and the literature may arise from differences in computational methodologies, basis sets, or functional choices, which are known to influence band gap predictions. Despite these variations, the overall trends remain consistent, reinforcing the reliability of our computational approach.

According to Table 3, the stability (in the sense of low reactivity) of the molecules can also be inferred, considering that the stability of a molecule is directly proportional to the value of the gap. Thus, the HOMO and LUMO energies for the most stable (less reactive) compound, limonene, were −6.32 and 0.35 eV, while for the least stable (more reactive) compound, α-phellandrene, the values were −5.72 eV and −0.68 eV. By subtracting the gaps of the more stable molecule from those of the less stable molecule, we obtained a variation of 1.63 eV, corresponding to 24.5% greater stability (lower reactivity) of limonene compared to α-phellandrene.

Furthermore, among the molecules, the gaps decrease in the following trend: limonene > sabinene > β-phellandrene > α-phellandrene. This trend suggests that α-phellandrene and β-phellandrene are the most reactive and polarizable molecules, as a smaller gap corresponds to higher reactivity and polarizability. When the electron cloud is easily polarized, the species is considered soft; when there is difficulty in polarization, the species is considered hard. Thus, if the species with which these structures will react are soft, the interaction is likely to be more favorable, *i.e.*, "soft acid" with "soft base" and "hard acid" with "hard base" [26,27].

It was observed that the α-phellandrene exhibits a higher HOMO energy, thus showing a greater electron-donating character compared to the other molecules. On the other hand, β-phellandrene has the lowest LUMO energy, meaning it is the most prone to accepting electrons. The HOMO and LUMO energies were also used to calculate the ionization potential, electron affinity, electronegativity, chemical hardness, chemical softness, and chemical potential, as shown in Table 4, thus characterizing the susceptibility of the molecules to attack by electrophiles and nucleophiles [13].

Table 3
HOMO and LUMO energies (in eV) for limonene, sabinene, α-phellandrene, and β-phellandrene.

Monoterpene	HOMO-2	HOMO-1	HOMO	LUMO	LUMO+1	LUMO+2
Limonene	−8.220	−6.724	−6.322	0.353	0.564	0.975
Sabinene	−8.173	−7.476	−6.235	0.345	0.894	1.389
α-phellandrene	−8.213	−7.923	−5.717	−0.676	1.024	1.415
β-phellandrene	−8.233	−7.940	−6.050	−0.692	0.855	1.343

Table 4
Ionization potential (IP), electron affinity (EA), electronegativity (χ), chemical potential (μ), hardness (η), softness (S), and polarizability (α), obtained for the optimized chemical structures of the hydrocarbon monoterpenes limonene, sabinene, α-phellandrene, and β-phellandrene using the theoretical model B3LYP/def2-TZVPP.

Molecule	IP	EA	χ	μ	η	S	α
Limonene	6.32	−0.353	2.98	−2.98	3.33	0.29	118.15
Sabinene	6.23	−0.345	2.94	−2.94	3.29	0.30	115.84
α-phellandrene	5.71	0.676	3.19	−3.19	2.52	0.39	119.09
β-phellandrene	6.05	0.692	3.37	−3.37	2.67	0.37	123.45

The HOMO-LUMO gap values indicate that monoterpenes with larger gaps, such as limonene, are more stable and less reactive, whereas smaller gaps in α-phellandrene and β-phellandrene suggest higher polarizability and reactivity. This trend is further supported by ionization potential and electron affinity values, where more stable molecules exhibit higher ionization potentials, making electron removal less favorable. At the same time, more reactive species have higher electron affinities, indicating a greater propensity to accept electrons.

The ionization potential for limonene is observed to be higher; thus, it exhibits greater hardness and lower softness among the molecules. Consequently, a larger amount of energy is required for the transition of an electron from the HOMO to the LUMO (larger gap), meaning that limonene is less likely to form cations quickly and is more susceptible to electrophilic attack. On the other hand, α-phellandrene presented the lowest ionization potential, indicating that this compound might present charge transfer mechanisms in a ligand–receptor interaction, and its ionic form may also exhibit biological activity [13].

Regarding electron affinity, the highest value was obtained for β-phellandrene, making it more prone to nucleophilic attack, and the anion formed will have lower energy than the neutral form, leading to the release of energy and increased stability. From the electronegativity values obtained, it is estimated that during an interaction, β-phellandrene will have a higher capacity to attract electrons and a lower tendency to lose them, as it presents a lower chemical potential. It is considered that the systems involved should reach a standard chemical potential at equilibrium. Furthermore, the chemical potential can be viewed as a potential for the flow of matter (similar to osmosis), phase changes, and chemical reactions [14].

The electronic properties of the investigated monoterpenes provide insights into their potential pharmacological applications. Compounds with lower HOMO-LUMO gaps, such as α-phellandrene and β-phellandrene, exhibit greater polarizability and reactivity, suggesting a stronger propensity for molecular interactions, which could enhance their biological activity. Moreover, higher electron affinity values indicate a greater tendency to participate in redox processes, a key factor in pharmacodynamics. These characteristics align with previous studies linking electronic properties to the bioactivity of essential oil components, reinforcing the potential of these monoterpenes as drug candidates.

3.6. Total density of states and projected density of states

Detailed analysis of the electronic structure of the $C_{10}H_{16}$ compounds was conducted using DOS and PDOS diagrams. The primary goal of this analysis is to understand the electronic structure of these compounds, identifying active sites and orbitals with the most significant influence on interaction processes. Additionally, the DOS study helps track variations in the electronic gap [28].

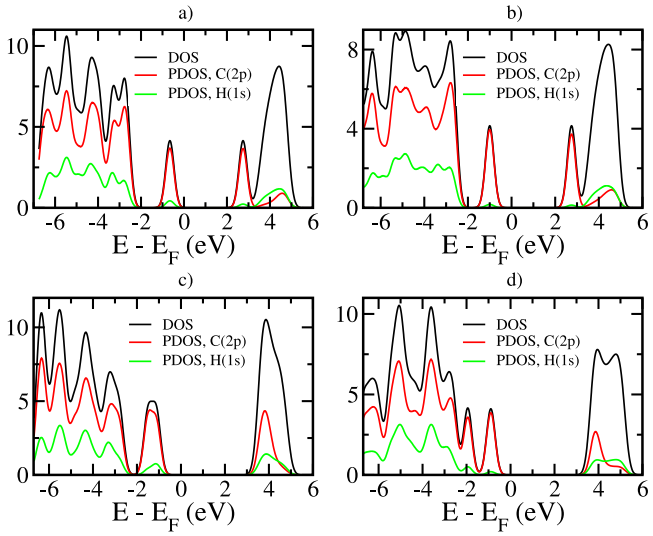

Fig. 5. DOS and PDOS of the hydrocarbon monoterpenes α-phellandrene (a), β-phellandrene (b), limonene (c), and sabinene (d) using the GGA-PBE functional. Partial contributions for s orbitals (green), $2p$ orbitals (red), and the total density of states (black line) are represented.

Fig. 5 presents the DOS and PDOS curves within the −6.8 eV range to 6.0 eV. The DOS highlights the electronic contributions with a gap consistent with the HOMO-LUMO energy values obtained for the studied molecules. In this context, it is noteworthy that limonene and sabinene exhibit the highest state contributions in the LUMO region, indicating a higher probability of accepting electrons and behaving as Lewis acids. Conversely, α-phellandrene and β-phellandrene molecules show greater state density in the HOMO region, revealing a stronger tendency to donate electrons and thus acting as Lewis bases.

Regarding the PDOS, the contributions from s and p orbitals are analyzed in detail. The red lines in Fig. 5 indicate the predominance of $2p$ orbitals in the energy levels below the Fermi level, as well as in the HOMO-LUMO gap region, suggesting that the main electronic contributions originate from carbon atoms. Furthermore, the observed gap is consistent with previous DOS and HOMO-LUMO results. This consistency reinforces the wide-bandgap semiconductor nature of the analyzed structures, indicating potential applications in developing bioelectronic devices [19,29,30].

The electronic properties of monoterpenes investigated in this study provide valuable insights into their reactivity and potential applications. While our analysis focuses on isolated molecules in the gas phase, monoterpenes can also form crystalline structures under specific conditions. Their optical and electronic responses could be further explored in such arrangements, including properties such as refractive index, transmittance, and reflectivity. Previous studies have demonstrated the importance of quantum-chemical descriptors in predicting the optical behavior of organic and hybrid materials, particularly in the context of crystal engineering and optoelectronic applications [31–34]. Future investigations into monoterpene-based molecular crystals could offer new perspectives for their potential use in photonic and electronic devices.

3.7. Thermodynamic properties

Another crucial factor is the variation in enthalpy (ΔH) associated with the process, which should be negative, zero, or slightly positive to ensure that the entropy variation (ΔS) is sufficient to yield a free energy variation (ΔG) less than zero, thereby achieving a spontaneous dissolution process [35].

For the isolated molecules, under constant pressure and temperature, we obtained total ΔH and ΔS values (in this order). For all the monoterpenes investigated, ΔH is approximately -2.45×10^{-5} kcal/mol. Additionally, both limonene and α-phellandrene exhibit ΔS = 29.42 kcal/mol, whereas sabinene has ΔS = 28.72 kcal/mol, and β-phellandrene has ΔS = 28.93 kcal/mol. Thus, these compounds' total ΔS is sufficient to produce a total ΔG value less than zero. For all molecules, ΔG is approximately -2.45×10^{-5} kcal/mol.

Considering that the ΔG values reflect the maximum chemical work these molecules can perform (such as muscular activity, bonding processes, and nerve signal transmission, among other biological reactions), lower ΔG values indicate a greater tendency for associations and reactions involving these molecules [35].

Another interesting feature is that these molecules are thermodynamically stable regarding the compounds from which they are formed. The ΔH values of formation indicate that the formation process of these molecules is spontaneous, releasing energy ($\Delta H°$ equal −148.5 kcal/mol, −137.23 kcal/mol, −149.42 kcal/mol, and −145.37 kcal/mol, limonene, sabinene, α- and β-phellandrene, respectively).

4. Conclusions

In this work, the quantum descriptors obtained provided a deeper understanding of the electronic effects and the physicochemical nature of the molecules limonene, sabinene, α-phellandrene, and β-phellandrene, which are hydrocarbon monoterpenes found in *Croton heliotropiifolius* Kunth. These findings enhance the information available to guide molecular recognition simulations and the search for compounds with diverse activities and applications. Structural analysis revealed the presence of optical isomerism, covalent bonds, and non-linear conformations. The sum of atomic charges was consistent with the total charge values and generally aligned with electronegativities, with minor deviations attributed to the calculation method. Additionally, Mulliken's analysis indicated a higher charge value for hydrogen atoms in β-phellandrene, suggesting a greater acidic character.

The resultant dipole moment confirmed the low polarity of these molecules, demonstrating solubility in non-polar or low-polarity solvents and highlighting potential electrophilic and nucleophilic sites. This alignment diverged from the electrostatic potential map only in the case of limonene. Thermodynamic data indicate that these molecules are reactive, as their total entropy is sufficient to yield a negative total free energy. Frontier orbital analysis showed that 99% of the electrons in these molecules occupy bonding orbitals, with only 1% in anti-bonding orbitals. The HOMO is predominantly bonding, rendering this region more susceptible to electrophilic attack, while the LUMO has anti-bonding characteristics, making it more vulnerable to nucleophilic attack.

Furthermore, limonene and sabinene exhibited the highest DOS in the LUMO region, indicating a higher probability of electron acceptance and behavior as Lewis acids. In contrast, α-phellandrene and β-phellandrene showed greater DOS in the HOMO region, suggesting a stronger tendency to donate electrons and act as Lewis bases. PDOS analysis indicated a predominance of $2p$ orbitals in the HOMO and LUMO regions, highlighting carbon atoms as the primary contributors to these orbitals.

The calculated gap values revealed that α-phellandrene and β-phellandrene are the most reactive and polarizable molecules, with a greater electron-donating character. Limonene exhibited the highest ionization potential, indicating greater hardness and lower softness, making it more susceptible to electrophilic attack. Conversely, α-phellandrene had the lowest ionization potential, suggesting potential charge transfer mechanisms in ligand–receptor interactions and the possibility of biological activity in its ionic form. Regarding electron affinity, β-phellandrene demonstrated the highest value, making it more prone to nucleophilic attack and more stable in its anionic form than in its neutral state.

Finally, in electronegativity, β-phellandrene is predicted to have a higher electron-attracting capacity and lower electron-repelling tendency during interactions, as it exhibits the lowest chemical potential.

These findings provide a foundation for screening and selecting monoterpene compounds for pharmaceutical applications. This study's electronic and thermodynamic properties can guide the rational design of new drug candidates derived from essential oils, optimizing their structural characteristics for enhanced bioactivity, stability, and bioavailability. Future investigations integrating molecular docking simulations will be essential further to explore these compounds' interaction with biological targets and refine their therapeutic potential.

CRediT authorship contribution statement

Maria Milena Regina E. Cavalcante: Writing – original draft, Methodology, Data curation, Conceptualization. **Rosemarie B. Marques:** Writing – original draft, Formal analysis, Data curation. **Ricardo R. Martins:** Writing – original draft, Formal analysis. **Evandro Paulo S. Martins:** Writing – original draft, Formal analysis. **Agmael M. Silva:** Writing – original draft, Methodology, Formal analysis, Data curation, Conceptualization. **Marcelo L. Pereira:** Writing – review & editing, Resources, Methodology, Funding acquisition, Formal analysis, Conceptualization. **Antonio de Macedo-Filho:** Writing – review & editing, Funding acquisition, Formal analysis, Data curation, Conceptualization.

Declaration of competing interest

The authors declare that they have no known competing financial interests or personal relationships that could have appeared to influence the work reported in this paper.

Acknowledgments

This work was partially supported by the Brazilian funding agencies CNPq and FAPDF. M.L.P.J. acknowledges financial support from the Research Support Foundation of the Federal District (FAP-DF, grant 00193-00001807/2023-16) and the National Council for Scientific and Technological Development (CNPq, grant 444921/2024-9). Thanks also to CENAPAD-SP (National High-Performance Center in São Paulo, State University of Campinas – UNICAMP, project: proj960) and NACAD (High-Performance Computing Center, Lobo Carneiro Supercomputer, Federal University of Rio de Janeiro – UFRJ, project: a22002) for the computational support provided. A.M.F. expresses gratitude to the Laboratory of Theoretical Physics and Computational Modeling (LFTMC), Teresina-PI, Brazil, and acknowledges support from the National Council for Scientific and Technological Development (CNPq), under grants 459961/2014-4 and 424950/2018-9.

Appendix A. Supplementary data

Supplementary material related to this article can be found online at https://doi.org/10.1016/j.comptc.2025.115138.

Data availability

Data will be made available on request.

References

[1] H.S. Elshafie, I. Camele, A.A. Mohamed, A comprehensive review on the biological, agricultural and pharmaceutical properties of secondary metabolites based-plant origin, Int. J. Mol. Sci. 24 (4) (2023) 3266.

[2] I. Süntar, Importance of ethnopharmacological studies in drug discovery: role of medicinal plants, Phytochem. Rev. 19 (5) (2020) 1199–1209.

[3] D.-C. Hao, P.-G. Xiao, Genomics and evolution in traditional medicinal plants: road to a healthier life, Evol. Bioinform. 11 (2015) EBO–S31326.

[4] J.M.T. de Alencar Filho, L.C. Araújo, A.P. Oliveira, G.A. L., A.G.M. Pacheco, F.S. Silva, L.S. Cavalcanti, A.M. Lucchese, J.R.G.S. Almeida, E.C.C. Araújo, Chemical composition and antibacterial activity of essential oil from leaves of croton heliotropiifolius in different seasons of the year, Rev. Bras. de Farm. 27 (2017) 440–444.

[5] P.K.A. Magalhães, E.N. Araujo, A.M. Santosa, M.B. Vandereic, C.C.L. Souza, M.S. Correia, S.A. Fonseca, M.A. Pavão, J.G. Costa, A.F. Santos, T.J. Matos-Rocha, Ethnobotanical and ethnopharmacological study of medicinal plants used by a traditional community in Brazil's northeastern, Braz. J. Biol. 82 (2022) e237642.

[6] C.B. Malafaia, A.C.S. Jardelino, A.G. Silva, A.J. de Souza, M.T.D.S. Correia, M.V. Silva, Effects of caatinga plant extracts in planktonic growth and biofilm formation in Ralstonia solanacearum, Microb. Ecol. 75 (2017) 555–561.

[7] R.G. Oliveira Junior, C.A.A. Ferraz, J.C. Silva, A.P. de Oliveira, T.C. Diniz, M.S. Gama, L.J. Quitans Junior, A.V.V. de Souza, U.S. dos Santos, I.C.C. Turatti, N.P. Lopes, V.P. Lorenzo, J.R.G.S. Almeida, Antinociceptive effect of the essential oil from croton conduplicatus Kunth (Euphorbiaceae), Molecules 22 (2017) 900.

[8] N.E. Thomford, D.A. Senthebane, A. Rowe, D. Munro, P. Seele, A. Maroyi, K. Dzobo, Natural products for drug discovery in the 21st century: innovations for novel drug discovery, Int. J. Mol. Sci. 19 (6) (2018) 1578.

[9] R.B. Marques, M.D.B. Sousa, W.S.S. Santos, N.F.B. Leite, E.M.S. Lima, A. Soares, C.L.S. Costa, F.A. Silva Filho, A. Maia Filho, E. Martins, R. Ramos, A. Macedo-Filho, Pharmacokinetic and toxicological prediction of the chemical constituents of the essential oil of the leaves of croton heliotropiifolius Kunth, J. Toxicol. Environ. Health 70 (2004) 066111.

[10] J.G. Moffat, F. Vincent, J.A. Lee, J. Eder, M. Prunotto, Opportunities and challenges in phenotypic drug discovery: an industry perspective, Nat. Rev. Drug Discov. 16 (8) (2017) 531–543.

[11] F.M. Araújo, M. Dantas, L.S. Silva, L.Y.S. Aana, I.F. Tavares, L.C. DE Souza Neta, Antibacterial activity and chemical composition of the essential oil of croton heliotropiifolius Kunth from Amargosa, Ind. Crop. Prod. 2008 (2017) 203–206.

[12] J.A. Rocha, N.C.S. Rego, B.T.S. CARVALHO, F.I. Silva, J.A. Sousa, R. Ramos, I.N.G. Passos, J. de Moraes, J.R.S.A. Leite, F.C.A. Lima, Computational quantum chemistry, molecular docking, and ADMET predictions of imidazole alkaloids of pilocarpus microphyllus with schistosomicidal properties, PLoS ONE 13 (2018) e0198476.

[13] A. Arroio, K.M. Honório, A.B.F. Silva, Propriedades Químico-Quânticas empregadas em estudos das relações estrutura-atividade, Quim. Nova 33 (2010) 694–699.

[14] W. Kohn, A.D. Becke, R.G. Parr, Density functional theory of electronic structure, J. Phys. Chem. 100 (1996) 12974–12980.

[15] NIM, PubMed central, 2024, URL https://pmc.ncbi.nlm.nih.gov/.

[16] K.-H. Ernst, Molecular chirality at surfaces, Phys. Status Solidi b 249 (2012) 1–32.

[17] S.E. Evans, B. Kasprzyk-Hordern, Applications of chiral chromatography coupled with mass spectrometry in the analysis of chiral pharmaceuticals in the environment, Phys. Status Solidi b 1 (2014) 34–51.

[18] F.D. Botelho, R.S.S.O. Oliveira, J.S.F.D.A. Almeida, T.C.C. França, I. Borges Junior, Comparação entre métodos para determinação de cargas atômicas em sistemas moleculares: N-N-(PTERINA-7-IL)CARBONILGLICIL - L-TIROSINA(NNPT), Quim. Nova 44 (2021) 161–171.

[19] F.A.R. Pereira, A. Macedo-Filho, A.M. Silva, N.F. Frazão, R.G. Sarmento, K.A.L. Lima, J.J.S. Melo, M.L. Pereira Junior, L.A. Ribeiro Junior, V.N. Freire, On the structural, electronic, and optical properties of L-histidine crystal: a DFT study, J. Mol. Model. 29 (2023).

[20] N.B. Robert, B.E.H. Sawaliho, K.K. Alain, The Oryzenin's effect on Di, tri and quadri-saccharide degradation. an investigation by a mixed method: ONIOM (DFT/B3LYP/6 -31 + G (d, p): AM1), Comput. Chem. 10 (2022) 97–119.

[21] S.G. Patra, R. Jha, H. Mondal, P.K. Chattaraj, Fischer and Schrock carbene complexes in the light of global and local electrophilicity-based descriptors, J. Phys. Org. Chem. 36 (12) (2023) e4337.

[22] K. Fukui, The role of frontier orbitals in chemical reactions (nobel lecture), Angew. Chem. Int. Ed. Engl. 21 (1982) 801–809.

[23] D.H. Pereira, L.C. Ducati, R. Rittiner, R. Custodio, A study of the rotational barriers for some organic compounds using the G3 and G3CEP theories, J. Mol. Model. 20 (2014) 2199–2464.

[24] R. Oses, M. Ferrando, F. Bruna, P. Retamales, M. Navarro, K. Fernández, W. Vera, M.J. Larrazábal, I. Neira, A. Paredes, et al., Exploring the Bioactive Potential and Chemical Profile of Schinus Molle Essential Oil: An Integrated in Silico and in Vitro Evaluation, Available At SSRN 5044461.

[25] N. Zeinali, I. Oluwoye, M.K. Altarawneh, M.H. Almatarneh, B.Z. Dlugogorski, Probing the reactivity of singlet oxygen with cyclic monoterpenes, ACS Omega 4 (9) (2019) 14040–14048.

[26] R.G. Pearson, Hard and soft acids and bases, J. Oftheamerican Chem. Soc. 85 (1963) 3533–3539.

[27] M.B. Procopio, A. Cesar, Polarizabilidades e primeira hiperpolarizabilidades elétricas dipolares de Ésteres e-4-amino-trans-1,3-butadienil-(1,2-di-hidroxibenzeno) de boro, alumínio e gálio, Quim. Nova 32 (2009) 1157–1163.

[28] S. Armaković, S. Armakvié, J. Setrajeié, S.K. Jaéimovski, V. Holodkov, Sumanene and its adsorption properties towards CO, CO2 and NH3 molecules, J. Mol. Model. 20 (2014) 2170–4624.

[29] S.R. Lázaro, E. Longo, A. Beltran, J.R. Sambrano, Propriedades eletrônicas e estruturais do PbTiO3: Teoria do Funcional Densidade aplicada a modelos periódicos, Quim, Nova 28 (2005) 10–18.

[30] J.G.S. Santos, A. Macedo-Filho, A.M. Silva, F.F. de Sousa, E.W.S. Caetano, M.B. da Silva, V.N. Freire, Computational structural, electronic and optical properties of the palmitic acid in its c form, J. Mol. Model. 27 (2021).

[31] L. Boulkaddat, A. Soussi, H. Najih, K. Abouabassi, N. Labchir, A. Elfanaoui, R. Markazi, K. Bouabid, A. Ihlal, et al., Experimental and theoretical study of electrodeposited CuInS2 thin films for solar cell applications, Phys. B 671 (2023) 415374.

[32] A. Soussi, R. Haounati, A. Ait hssi, M. Taoufiq, A. Asbayou, A. Elfanaoui, R. Markazi, K. Bouabid, A. Ihlal, First principle study of structural, electronic, optical properties of Co-doped ZnO, J. Compos. Sci. 7 (12) (2023) 511.

[33] M. Taoufiq, A. Soussi, A. Elfanaoui, S. Baoubih, A. Ihlal, K. Bouabid, et al., DFT theoretical and experimental investigations of the effect of Cu doping within SILAR deposited Zns, Opt. Mater. 147 (2024) 114607.

[34] A. Soussi, R. Haounati, M. Taoufiq, S. Baoubih, Z. Jellil, A. Elfanaoui, R. Markazi, A. Ihlal, et al., Investigating structural, morphological, electronic, and optical properties of SnO2 and al-doped SnO2: A combined DFT calculation and experimental study, Phys. B 690 (2024) 416242.

[35] C.R. Martins, W.A. Lopes, J.B. Andrade, Solubilidade das Substâncias Orgânicas, Quim. Nova 36 (2013) 1248–1255.